Size and shape of molecular ions and their relevance to the packing of the 'soft salts'

Andrew L. Rohl* and D. Michael P. Mingos**,†
Inorganic Chemistry Laboratory, University of Oxford, South Parks Road, Oxford OX1 3QR (UK)

(Received November 2, 1992, revised March 8, 1993)

Abstract

The manner in which inorganic molecules and ions pack in the solid state is critical in determining their conductivity, magnetic and non-linear optical properties. In a previous paper the methodology for calculating the volumes, surface areas, effective radii and shapes of inorganic ions was developed. In this paper these structural parameters are used to rationalise the solid state structures of 'soft salts' which consist of a large cluster cation and a large cluster anion. The effective radii of the cluster ions derived from the volume contained within the van der Waals sphere of their atoms may be used to calculate radius ratios for the salts which may be used to interpret the observed solid state structures. The distortions from the idealised inorganic salt structures have been related to the non-spherical nature of the ions, which have been calculated from their moments of inertia. The differences in the ion environments of those salts which have more than one crystal modification have been explored using potential energy calculations.

Introduction

The 'soft salts' are salts which consist of a large cluster cation and a large cluster anion. They were first synthesised by Green *et al.* [1] who made four compounds: $[Mo_4(\mu\text{-}C_5H_4Pr^i)_4(\mu^3\text{-}S)_4]_2[Os_6(CO)_{18}]$ (**2**), $[Fe_4(\mu\text{-}C_5H_5)_4(\mu^3\text{-}S)_4][Fe_4(NO)_4(\mu^3\text{-}S)_4]\cdot(CH_3)_2CO$ (**3**), $[Fe_4(\mu\text{-}C_5H_4Me)_4(\mu^3\text{-}S)_4][Fe_4(NO)_4(\mu^3\text{-}S)_4]$ (**4**) and $[Mo_4(\mu\text{-}C_5H_4Pr^i)_4(\mu^3\text{-}S)_4][Fe_4(NO)_4(\mu^3\text{-}S)_4]$ (**5**). These compounds were structurally determined by Prout and co-workers [2] who found that salts **2** and **5** both crystallise in two different phases. An additional soft salt, viz. $[Rh_3(\mu^3\text{-}PMe)(PMe_3)_4(CO)_5][FeRh_5(PMe_3)(CO)_{15}]$ (**1**) has subsequently been reported by Podlahová *et al.* [3].

Green *et al.* were interested in the crystal packing properties of the cluster soft salts because they are relevant to their interesting conductivity and electronic bulk properties. They concluded from rather crude estimates of the cation and anion radii that the structures of the salts could not be readily interpreted in terms of radius ratio rules [1]. Specifically they noted that although the salts **2** and **5** had very different solid state structures, their calculated radii were essentially identical.

Although the molecular design of solid state materials which optimise conductivity, magnetic and non-linear optical properties will prove to be an increasingly important concern for inorganic chemists [4], our understanding of packing effects remains at a very primitive stage of its development. There have been surprisingly few attempts to model the packing modes of inorganic and organometallic molecular compounds [5] and salts [6, 7]. Recently, we have examined the packing in $[PF_6]^-$ salts as a function of cation size, shape and charge [8].

In this paper we examine the packing modes of the soft salts reported by Green and Podlahová using parameters which describe the size and shape of the constituent ions. Atom–atom potential methods are used to try and determine the differences between the different crystal modifications for salts **2** and **5**.

Calculation methods

In a previous paper [9] the basic procedures for calculating the volumes (V_m), surface areas (S_m), moments of inertia (M_1, M_2, M_3) and effective radii (R_{eff}) of cations and anions were described in detail. The method used to calculate the volume is that of Gavezzotti [10]. The effective radius is defined from the volume by the expression:

*Present address: Royal Institution of Great Britain, 21 Albemarle St, London W1X 4BS, UK.
**Present address: Department of Chemistry, Imperial College of Science, Technology and Medicine, South Kensington, London SW7 2AY, UK.
†Author to whom correspondence should be addressed.

0020-1693/93/$6.00
© 1993 – Elsevier Sequoia. All rights reserved

$$R_{eff} = \sqrt[3]{\frac{3V_m}{4\pi}}$$

The shape parameters are derived from the moments of inertia calculated without mass weighting [11]. Three indices were defined, F_s, F_c and F_d which measure how close an ion is to spherical, cylindrical and discoidal geometries, respectively. The closer the values of the parameters are to unity, the closer the ion is to the geometry represented by the parameter. These ionic shapes can be best visualised by representing them as ellipsoids with axis lengths proportional to the moments of inertia [8]. The arrangement of anions about a cation or vice versa where either the anion or cation is non-spherical can then be seen by displaying these ellipsoids using a thermal ellipsoid plotting program [12]. A computer program, which calculates these size and shape quantities is available. It is written in C and runs on Apple Macintosh Computers.

The difference between the cation environments for the two crystalline forms has been placed on a more quantitative basis by determining the intermolecular potential energy between a cation and its anion nearest neighbours. There will be two contributions to the energy, one corresponding to van der Waals and repulsive forces and the other to electrostatic interactions. The parameters for the former term are readily available for the non-metallic elements and were taken from the OPEC program of Gavezzotti [10]. For the first row transition metals the values used were those of Kr and for the second and third rows those of Xe [13] were utilised. The atomic charges were obtained from Extended Hückel (EHT) calculations [14]. Although the charges from EHT calculations are not completely reliable, the size of these clusters as well as the presence of transition metals and unpaired electrons make these ions unsuitable for more rigorous techniques such as CNDO or *ab initio* methods. Another justification for the use of the EHT method is that we are comparing results between systems with the same constituent ions and so it is the relative charges which are important not the absolute values.

Results and discussion

The size and shape parameters described above have been calculated for the soft salts and are listed in Table 1. The salts **2** and **5** which crystallise in alternative space groups have had their parameters calculated for the ions in both modifications. The calculated volumes, V_m, of the ions range from 206 Å^3 for $[Fe_4(NO)_4(\mu^3\text{-}S)_4]^-$ to 603 Å^3 for $[Mo_4(\mu\text{-}C_5H_4Pr^i)_4(\mu^3\text{-}S)_4]^+$. These volumes may be used to estimate effective radii for these ions, R_{eff}. These calculations are based on the assumption that the ions are spherical. The moments of inertia given in the Table and associated shape indices F_s, F_c and F_d suggest that this is a particularly good assumption for $[Os_6(CO)_{18}]^{2-}$ and $[Fe_4(NO)_4(\mu^3\text{-}S)_4]^-$ and a reasonable assumption for $[Fe_4(\mu\text{-}C_5H_5)_4(\mu^3\text{-}S)_4]^+$ and $[Fe_4(\mu\text{-}C_5H_4Me)_4(\mu^3\text{-}S)_4]^+$. $[Mo_4(\mu\text{-}C_5H_4Pr^i)_4(\mu^3\text{-}S)_4]^+$ has distinct discoidal and cylindrical components in some of its conformations whilst the Podlahová soft salt ions are the least spherical of the ions investigated. In the soft salt series there is a large duplication in the ions used. As a result the structure of each ion has been crystallographically determined many times. The results in Table 1 indicate that the calculated volume and surface area parameters of an ion are essentially constant between structures but the moments of inertia can vary significantly. The biggest change has been observed in the shape parameters of $[Mo_4(\mu\text{-}C_5H_4Pr^i)_4(\mu^3\text{-}S)_4]^+$. The calculated moments of inertia, which estimate the shape, vary from 791, 588, 551 Å^2 in **2a** to 905, 532, 501 Å^2 in **5a**. The parameters F_s, F_c and F_d, which estimate the spherical, cylindrical and discoidal aspects of the structure, clearly indicate that the cation in **2a** is more spherical. The sum of the moments of inertia for an ion is basically constant (for $[Mo_4(\mu\text{-}C_5H_4Pr^i)_4(\mu^3\text{-}S)_4]^+$ the average sum is 1943 with a standard deviation of 20). This is because the sum of the moments is dependent only on the number of atoms in an ion and their distances from the ion centroid, whereas the individual moments are dependent on the spatial arrangement of the atoms.

Table 1 also provides the R_{max} radii for the ions, which is the maximum dimension of the ion from its centroid. In general the ratio R_{eff}/R_{max} provides an estimate of the degree of interpenetration of an ion with its counterion within the crystal structure. The values given in Table 1 range from 0.62 to 0.80 suggesting that interpenetration of the cation and anion van der Waals surfaces in soft salts will not be negligible.

A comparison of the packing coefficients (C_k) between the different phases of **2** and **5** shows that a reduction in the symmetry of the space group leads to an increase in the packing density, an observation which has been noted previously for organic crystals by Kitaigorodsky [15].

The structures of the salts are discussed primarily in terms of the *a*/*c* ratio, i.e. R_{eff}(anion)/R_{eff}(cation). The ratio varies from 0.99 in $[Rh_3(\mu^3\text{-}PMe)(PMe_3)_4(CO)_5][FeRh_5(PMe_3)(CO)_{15}]$ (**1**) to 0.70 in $[Mo_4(\mu\text{-}C_5H_4Pr^i)_4(\mu^3\text{-}S)_4][Fe_4(NO)_4(\mu^3\text{-}S)_4]$ (**5**) and is reflected in a change in the structure type. The structure type of a salt can often be deduced from an examination of the coordination numbers (*CN*s) of the cations and anions in the salt. We have defined the coordination

TABLE 1. Size and shape parameters of the cluster cations and cluster anions of the 'soft salts'

Salt	Ion	Space group	a/c	V_m (Å^3)	S_m (Å^2)	R_{eff} (Å)	R_{max} (Å)	R_{eff}/R_{max}	M_1 (Å^2)	M_2 (Å^2)	M_3 (Å^2)	F_s	F_c	F_d	C_k (%)
1	$[Rh_3(\mu^3\text{-PMe})(PMe_3)_4(CO)_5]^+$	*Pnma*	0.99	497	546	4 91	7.15	0.69	614	445	278	0.45	0.41	0.47	65.2
	$[FeRh_5(PMe_3)(CO)_{15}]^-$			475	478	4.84	6.74	0.72	392	196	186	0 47	0.51	0.37	
2a	$[Mo_4(\mu\text{-}C_5H_4Pr^i)_4(\mu^3\text{-S})_4]^+$	*C2/c*	0.92	603	632	5.24	8.04	0.65	791	588	551	0.70	0.28	0.20	67.3
	$[Os_6(CO)_{18}]^{2-}$			467	453	4.81	6 02	0.80	201	200	195	0.97	0.01	0.02	
2b	$[Mo_4(\mu\text{-}C_5H_4Pr^i)_4(\mu^3\text{-S})_4]^+$	$P2_1/a$	0.92	603	633	5.24	8.32	0.63	847	673	459	0.54	0.33	0.40	68.3
	$[Mo_4(\mu\text{-}C_5H_4Pr^i)_4(\mu^3\text{-S})_4]^+$			602	635	5.24	8.16	0.64	805	585	558	0.69	0.29	0.20	
	$[Os_6(CO)_{18}]^{2-}$			466	453	4.81	6.02	0.80	200	197	194	0.97	0 02	0.02	
3	$[Fe_4(\mu\text{-}C_5H_5)_4(\mu^3\text{-S})_4]^+$	$P\bar{1}$	0.81	384	390	4.51	5.71	0.79	303	213	173	0.57	0.36	0.33	70.2
	$[Fe_4(NO)_4(\mu^3\text{-S})_4]^-$			207	229	3.67	5.91	0.62	54	50	49	0.90	0.09	0.07	
	$(CH_3)_2CO$			61	88	2.45	3.32	0.74	19	7	3	0.16	0.74	0.76	
4	$[Fe_4(\mu\text{-}C_5H_4Me)_4(\mu^3\text{-S})_4]^+$	$P2_1/c$	0.77	444	461	4.73	6 93	0.68	383	339	254	0.66	0.23	0.30	69.6
	$[Fe_4(\mu\text{-}C_5H_4Me)_4(\mu^3\text{-S})_4]^+$			446	465	4.74	6.92	0.68	347	319	306	0.88	0.10	0.08	
	$[Fe_4(NO)_4(\mu^3\text{-S})_4]^-$			206	228	3.66	5.88	0 62	53	50	49	0.93	0.06	0.05	
	$[Fe_4(NO)_4(\mu^3\text{-S})_4]^-$			207	229	3.67	5.89	0.62	52	51	50	0.97	0.02	0.03	
5a	$[Mo_4(\mu\text{-}C_5H_4Pr^i)_4(\mu^3\text{-S})_4]^+$	*Pbcn*	0.70	599	627	5.23	8.21	0.64	905	532	501	0.55	0.43	0.30	68.1
	$[Fe_4(NO)_4(\mu^3\text{-S})_4]^-$			207	229	3.67	5.89	0.62	54	51	48	0.89	0.08	0.08	
5b	$[Mo_4(\mu\text{-}C_5H_4Pr^i)_4(\mu^3\text{-S})_4]^+$	$P2_1/n$	0.70	600	631	5.23	8.48	0.62	892	592	436	0.49	0.42	0.41	70.4
	$[Fe_4(NO)_4(\mu^3\text{-S})_4]^-$			207	229	3.67	5.92	0.62	56	51	46	0 82	0.14	0.14	

number of a cation as the number of anions which are closer than the nearest neighbour cation to this cation. The coordination number of the anion is defined similarly. For centroid–centroid distances for the soft salts see 'Supplementary material'. For a 1:1 simple inorganic salt the coordination numbers of both the cation and anion are equal. For many of the soft salts the coordination numbers of the anion and cation returned by our algorithm differ. Often these salts have structures based on simple inorganic structure types but irregularities in the surface shapes of the ions causes deviations to occur resulting in unusual coordination numbers. In these cases the structure type can be deduced by examining the distribution of cation–anion inter-ion distances. If there is a large gap between the sixth and seventh cation–anion distances then the structure type will most likely be a distortion of a simple inorganic salt with cations coordinated to six anions, i.e. NaCl or NiAs. A large gap between the eight and ninth cation–anion distances suggests a structure type based on eight-coordination, *e.g.* salt **1** has a cation *CN* of 5 and an anion *CN* of 4 but in the cation–anion distance list there is a large gap between the eight (12.5 Å) and ninth (15.9 Å) nearest neighbours indicating a structure type based on eight-coordination. Further clues to the structure type are given by the cation–cation and anion–anion distances of this salt which both show gaps between the sixth and seventh distances. This suggests that the structure is based on CsCl, the six cation–cation nearest neighbours lying at the faces of the cube of anions arranged about a cation.

In the following sections we shall examine the structure of each salt in more detail.

$[Rh_3(\mu^3\text{-PMe})(PMe_3)_4(CO)_5][FeRh_5(PMe_3)(CO)_{15}]$ (1)

The *a/c* ratio of this salt is 0.99 and its structure may be described as distorted CsCl. The structure is represented by a sphere packing diagram in Fig. 1. The structure reflects the non-spherical nature of the cation and anion and results in the large spread of nearest neighbour cation–anion distances of 8.6–12.5 Å. The Rh_3 triangle of the cation lies approximately in the plane between two opposite edges of the cube with the capping PMe group directed towards an anion. There is interlocking between CO groups on neigh-

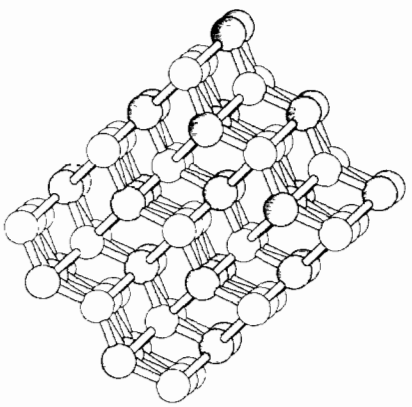

Fig. 1. The sphere packing diagram of **1** illustrating its distorted CsCl structure The darker spheres represent the anions and the lighter spheres the cations.

bouring anions along four edges of the cube, which produces a distorted cube with six anions closer to each other than the other two. This is clearly visible in Fig. 1. This is responsible for the large spread in nearest neighbour distances since the cation is too large to allow the remaining two anions to interpenetrate with the other six.

$[Mo_4(\mu\text{-}C_5H_4Pr^i)_4(\mu^3\text{-}S)_4]_2[Os_6(CO)_{18}]$ (2a) (2b)

This salt crystallises in the two space groups *C2/c* and $P2_1/a$ but the packing arrangements in both structures are very similar. The calculated *a/c* ratio of 0.92 is similar to that calculated for **1** and therefore eight-coordination is anticipated in the solid state. The change in stoichiometry from AB to A_2B suggests that an antifluorite (8:4) structure might be adopted. A distorted antifluorite structure is indeed observed in both modifications, a result noted previously by Green *et al.* The packing arrangement is illustrated schematically for both modifications in Fig. 2. The small differences in the packing arrangements are associated with small differences in the conformations of the two cations as indicated by the calculated moments of inertia in Table 1. These differences correspond to rotations of the CpPr^i rings and conformational differences in the isopropyl group itself. The cation–anion distances range from 8.7 to 10.1 Å in **2a** and from 8.4 to 10.2 Å in **2b**. The arrangement of the four anions about a cation for **2a** is displayed in Fig. 3. The four anions lie above the four sulfur atoms of the cubane, providing a much more compact structure to that which would be obtained if the anions lay above the CpPr^i rings. The closest contacts to the sulfur atoms occur via a triangle of oxygen atoms from an $Os(CO)_3$ group on each anion. The sum of the ion radii, $R_{eff}(c+a) = 10.0$ Å lies towards the top end of the observed range of cation–anion distances reflecting this. This emphasises the way in which the cations and anions interlock with each other because their van der Waals surfaces of complex ions are not spherical but contain protrusions and indentations.

The environments of the two independent cations in the second modification are similar, the primary difference being that in **2b** one of the anions is rotated by about 90° relative to the other three. The cation nearest neighbours for both forms of $[Mo_4(\mu\text{-}C_5H_4Pr^i)_4(\mu^3\text{-}S)_4]_2[Os_6(CO)_{18}]$ are reproduced using shape ellipsoids in Fig. 4. All the cations are oriented with their largest axes horizontal. The rotation of one anion in **2b** with respect to the other three can be clearly seen. The position of the cations within the tetrahedra also differ with cation 1 having its longest axis lying along an edge of its tetrahedron whilst cation 2 has its longest axis lying in a face of its tetrahedron. This difference is reflected in the average cation–anion nearest neighbour distance which is 9.40 Å for cation 1 and 9.30 Å for cation 2. The cation in form **2a** has its longest axis lying along the edge of its anion tetrahedron resulting in an average cation–anion nearest neighbour distance of 9.44 Å, similar to the result for cation 1 of form **2b**.

The cation energies due to the nearest neighbour anions have been calculated using a slightly modified version of the OPEC program [10]. For the calculated atomic charges used in the calculation as well as the

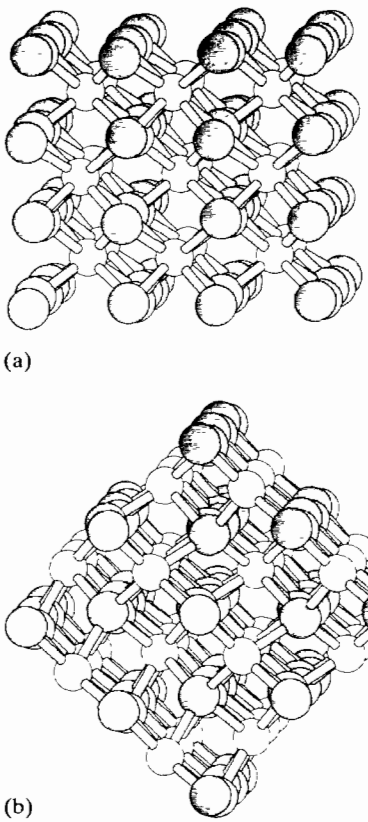

Fig 2 The sphere packing diagrams of (a) **2a** and (b) **2a** revealing that they both adopt distorted antifluorite structures.

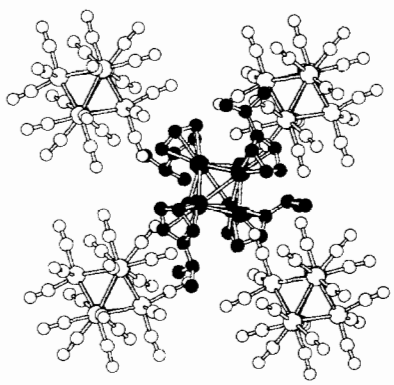

Fig. 3 The disposition of the four nearest neighbour anions about a cation in **2a**

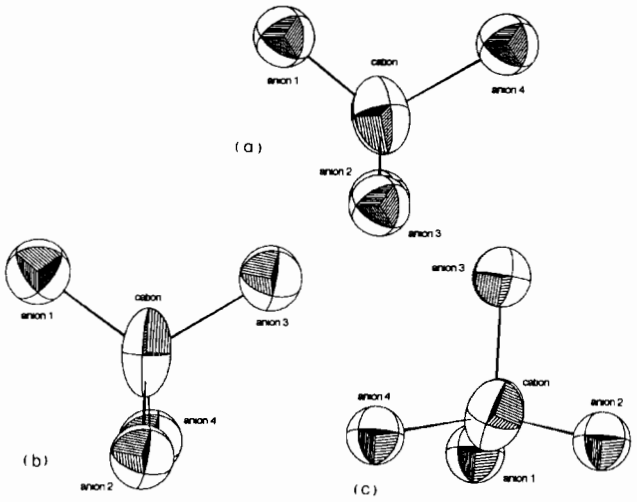

Fig. 4. Ellipsoid diagrams showing the nearest neighbour anion positions around a cation in (a) **2a** and (b, c) **2b** The larger the anion number, the further it is from the cation

energies listed by contact type and the results for **5**, see 'Supplementary material'. The total energies for the different cations are very similar (-1261 kJ mol^{-1} for **2a**, -1277 kJ mol^{-1} for cation 1 and -1294 kJ mol^{-1} for cation 2 in **2b**) as expected for two phases of the same material. The energies of the two cations in form **2b** are less then that found for **2a** showing that the former is packed more efficiently. The total energies of the three cations would be expected to become even closer in value were the shell of nearest neighbour cations included in the calculation since they are closer in form **2b** than form **2a** and hence more repelling. If only the van der Waals interactions are included, it is striking that cation 2 in **2b** is actually higher in energy than **2a**. This is caused by repulsions between the surface hydrogens on the cation and carbonyl groups on the anions. This is more than counterbalanced, however, by the gain in energy due to the increased electrostatic interactions. Both of the cations in **2b** show increased molybdenum van der Waals interactions with the anions relative to **2a** but cation 2 in **2b** shows decreased sulfur van der Waals interactions relative to the other two cations. Note that the stabilisation of **2b** over **2a** corresponds to small differences in each individual interaction, i.e. there is no one interaction either electrostatic or van der Waals which dramatically changes from form **2a** to **2b**.

$[Fe_4(\mu\text{-}C_5H_5)_4(\mu^3\text{-}S)_4][Fe_4(NO)_4(\mu^3\text{-}S)_4]\cdot(CH_3)_2CO$ (3)

This soft salt crystallises with a molecule of acetone in the asymmetric unit and therefore it was of interest to examine the way in which the packing is influenced by the incorporation of solvent molecules. A comparison of the R_{eff} values of the components of this salt (see Table 1) shows that even when dealing with large cluster cations and anions, the relative size of the solvent molecule is not insignificant. Hence, it is unlikely that a salt containing some solvent will adopt a structure similar to that adopted if the solvent was not present, with the solvent occupying gaps left in the solvent free structure. Figure 5 schematically illustrates the structure actually adopted by salt **3**. The incorporation of the solvent molecules has had a dramatic effect, producing a layer structure rather than an NiAs or NaCl type structure predicted by the *a/c* ratio. The layers of acetone molecules separate the structure into double layers of $[Fe_4(\mu\text{-}C_5H_5)_4(\mu^3\text{-}S)_4][Fe_4(NO)_4(\mu^3\text{-}S)_4]$ in which both the anions and cations have a coordination number of four, based on very distorted tetrahedra. The tetrahedra about the cation has an average vertex–centroid–vertex angle of 104° with a standard deviation of 26°. The corresponding values for the anion are 101 and 28°.

$[Fe_4(\mu\text{-}C_5H_4Me)_4(\mu^3\text{-}S)_4][Fe_4(NO)_4(\mu^3\text{-}S)_4]$ (4)

This salt which crystallises in the space group $P2_1/c$ has two independent cations and anions in the asymmetric unit. The *a/c* ratio is calculated to be 0.77 and is thus near the minimum radius ratio for eight-coordination (0.73). In fact a coordination number of six is actually adopted and the structure is best described as distorted anti-nickel arsenide as illustrated schematically in Fig. 6. The six cation–anion distances lie between 7.2–9.0 and 7.2–8.7 Å for the two modifications

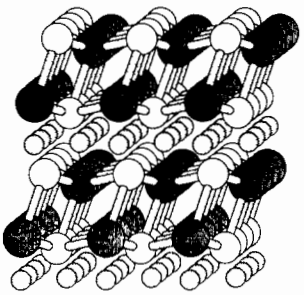

Fig 5 The sphere packing diagram of **3** clearly showing the formation of a layer of solvent molecules (intermediate colour spheres)

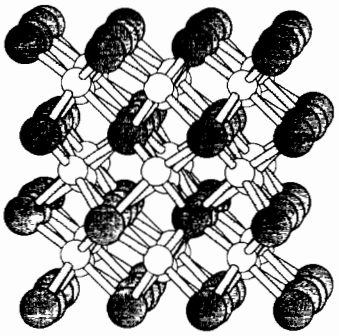

Fig 6. The sphere packing diagram of **4** depicting its anti-NiAs structure

which is a comparatively narrow range indicating that the distortions from an ideal anti-NiAs structure are small. The calculated $R_{eff}(c-a)$ is 8.4 Å which in common with **2a** and **2b** lies at the higher end of the range indicating that significant interpenetration between the cation and anion is occurring.

The anions which form a distorted trigonal prism around the first modification of the $[Fe_4(\mu\text{-}C_5H_4Me)_4(\mu^3\text{-}S)_4]^+$ cation are illustrated in Fig. 7. A very similar arrangement is obtained for the second modification. In the Figure, two of the CpMe groups on the cation are directed towards the back edges of the two horizontal trigonal faces. These edges are the two longest in the trigonal prism. This arrangement leaves the other two CpMe groups on the cation lying at the middle of two large square faces. This is possibly the reason why an anti-NiAs structure is being adopted in preference to a NaCl structure since a CpMe group needs a large face to fit in and an octahedron with large enough faces to accommodate a CpMe group would be much larger than the trigonal prism adopted, leading to a low packing coefficient. This preferred adoption of NiAs structures over NaCl structures for ions with ring systems has also been shown to occur in hexafluorophosphate salts [8].

The position of the anion relative to the cation octahedron is uncomplicated. One NO group on the anion is directed at the middle of one the top face of the antiprism leaving the other three NO groups at the middle of three of the four equatorial faces.

$[Mo_4(\mu\text{-}C_5H_4Pr^i)_4(\mu^3\text{-}S)_4][Fe_4(NO)_4(\mu^3\text{-}S)_4]$ (5a) (5b)

This soft salt crystallises in the space groups *Pbcn* and $P2_1/n$. Green *et al.* reported that the two phases had different structures, one based on a cation with four-coordination and the other with a cation coordination number of five. A more detailed study of these structures has shown that they have very similar solid state structures based on the unusual coordination number of five. The calculated *a/c* ratio is 0.70 and is consistent with the adoption of a low coordination number. It is worth noting that the *a/c* ratio reported in this work is rather different to the value of 0.78 reported by Green *et al.* Although their method of estimating the radius of an ion is not explicitly described, it is clear that it is proportional to the quantity R_{max}, i.e. the largest distance between the centroid of the ion and its outer surface. This is a rather crude radius to use since it depends solely on the length of the ligands present in the ion and takes no account of the number of ligands present. In the $[Fe_4(NO)_4(\mu^3\text{-}S)_4]$ anion most of the space around the metal–sulfur cube is accessible to cations so R_{max} will lead to an overestimate of the anion's size. R_{eff} on the other hand averages out the ligand contributions over the whole surface leading to a much more realistic radius.

The schematic packing diagrams of both structures are illustrated in Fig. 8. These show that the observed structures do not correspond to that observed previously

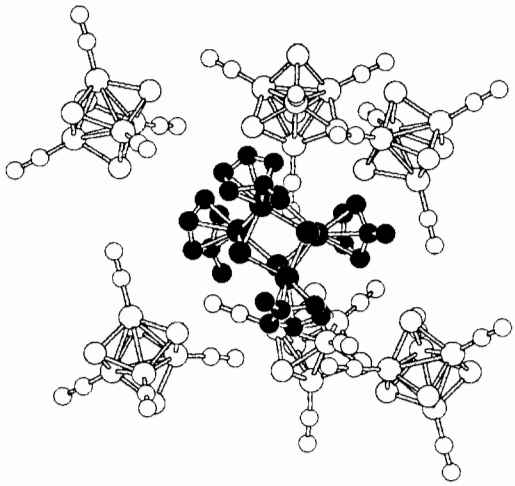

Fig. 7. The trigonal prismatic arrangement of anions around a cation in **4**

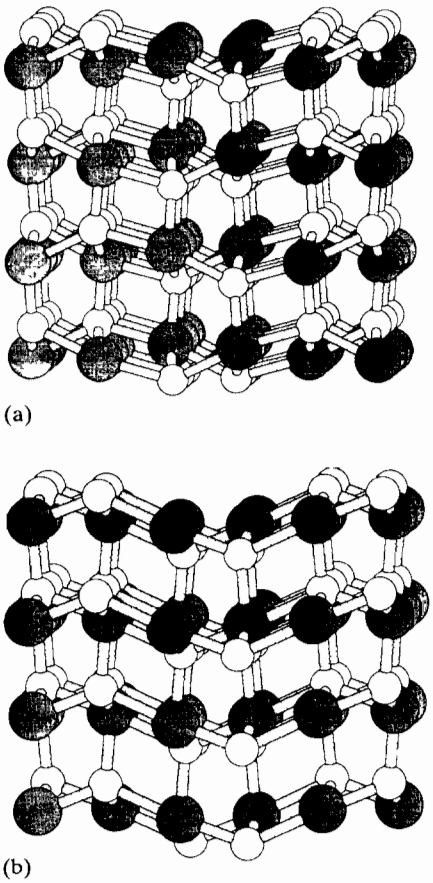

Fig. 8. The sphere packing diagrams of (a) **5a** and (b) **5b** revealing that they both adopt a novel structure based on five-coordinated anions and cations

for any simple salts. The anions adopt a distorted square pyramidal coordination environment and the cations a very distorted trigonal bipyramidal environment. The cation–anion distances range from 7.4 to 8.6 Å in **5a** and from 7.7 to 8.9 Å in **5b**. The $R_{\text{eff}}(c+a)$ sum is 8.9 Å, suggesting that significant interpenetration is occurring in these structures.

The cation environments of **5a** and **5b** seem quite different. Although the relative positions of the ions is similar, the relative orientations appear quite different. This can be most easily seen in the ellipsoid representations shown in Fig. 9. For **5a** the long axis of the anion is almost in the equatorial plane whilst for **5b** the long axis of the cation lies in one of the triangular faces of the trigonal bipyramid. This would suggest that **5b** should pack tighter than **5a** which is manifest in the higher packing coefficient observed for the former. The full cation environments in the same projections as that for the ellipsoid representations are reproduced in Fig. 10. In Fig. 10(a) two of the CpPr' groups on the cation lie at the middle of two of the equatorial edges of the trigonal bipyramid. This leaves the two remaining CpPr' groups lying in the positions normally occupied by the apiecs of a trigonal bipyramid. Hence the two apical anions are located at about 60° to the trigonal plane accounting for the large deviations of the cation coordination polyhedron from an ideal trigonal bipyramid. Figure 10(b) shows that only one CpPr' group on the cation in the second modification lies at the middle of an equatorial edge of the trigonal bipyramid. One of the other CpPr' group lies at the bottom of the Figure hindering one of the anions, leaving the last two such that the top apical anion lies between them. This explains why the second modification has one large cation–anion distance compared to the two found for the first modification.

The energies of the two different environments are very similar (-889 kJ mol^{-1} for **5a** and -912 kJ mol^{-1} for **5b**), as was found for $[Mo_4(\mu\text{-}C_5H_4Pr')_4(\mu^3\text{-}S)_4]_2[Os_6(CO)_{18}]$. Again the structure with the lower

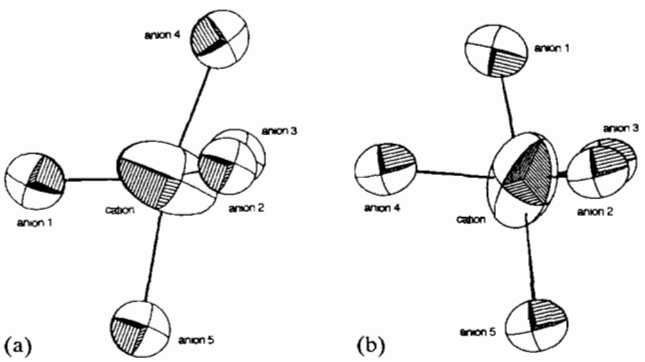

Fig. 9. Ellipsoid representation of the arrangements of anions about a cation in (a) **5a** and (b) **5b**

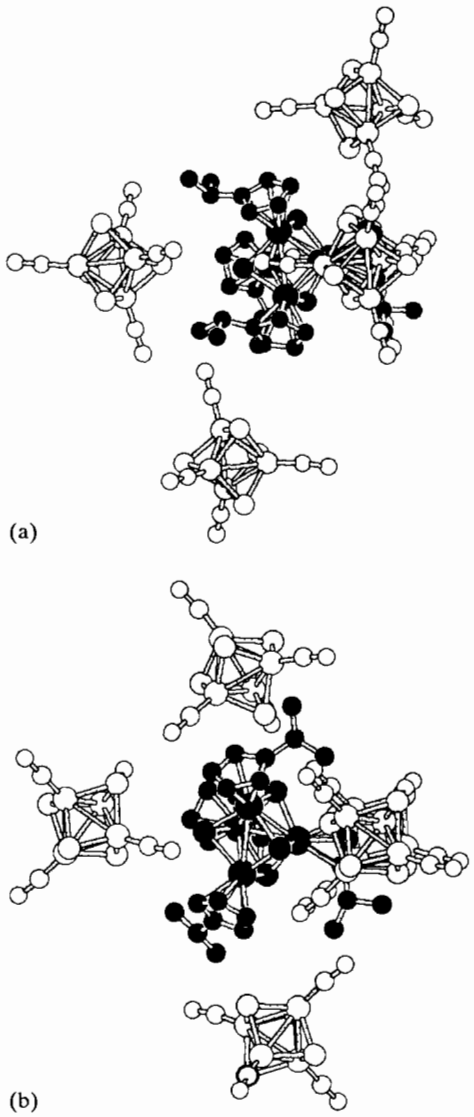

Fig 10. The arrangement of anions about a cation for (a) **5a** and (b) **5b** in the same projection as Fig. 9.

symmetry has the lower energy. In contrast to **2**, the cation in **5b** has a lower energy than cation **5a** if only van der Waals interactions are included. This can be rationalised in terms of the larger charge on the anion in **2** making van der Waals repulsion between surface atoms more favourable than that experienced by surface atoms in **5**. Note however that some repulsions between the surface hydrogens on the cation and nitrosyl groups on the anions is occurring in **5b**. The only other van der Waals interactions which are more pronounced in **5a** than **5b** are the S–S interactions. This along with the much larger S–H interactions present in **5b** compared to **5a** suggest that the cation in **5b** is oriented with its CpPr' groups interacting more strongly with the anions than that found for **5a**, sacrificing some S–S interactions, leading to a more stable structure. These trends are also mirrored in the calculated electrostatic energies.

Conclusions

The results of the packing analysis for the 'soft salts' are summarised in Table 2. The dimensional and shape parameters have been useful for accounting for some of the cruder aspects of the packing modes in these crystalline solids. In particular there appears to be a good relationship between the calculated *a/c* ratios and the observed coordination numbers in the solid state crystal structures. Eight coordinate CsCl and anti-fluorite structures were observed when *a/c* lay between 0.99 and 0.93. An anti-nickel arsenide structure was observed for $[Fe_4(\mu\text{-}C_5H_4Me)_4(\mu^3\text{-}S)_4][Fe_4(NO)_4(\mu^3\text{-}S)_4]$ where $a/c = 0.78$ and an unusual 5:5 packing mode based on distorted trigonal bipyramidal and square pyramidal coordination geometries were observed when $a/c = 0.71$.

These results suggest that the relative sizes of the ions in the soft salts is the primary factor in determining their solid state structures. The observed structures all show significant distortions away from the idealised structures of simple ionic salts, because of deviations from the ideal spherical shape due to the presence of protrusions and indentations on the surfaces of the ions. The degree of non-sphericality has been estimated by the moments of inertia calculations and by comparisons of the observed centroid–centroid distances with the sum of R_{eff} for cation and anion. An examination of cation environments indicates that the anions adopt positions around the cation which maximise the van der Waals contacts.

One salt in this study had solvent of crystallisation in its lattice. The solid state structure was found not to be based on that of any simple inorganic salt. The large size of the solvent relative to the cluster anion and cluster cation ensured that it was unable to be incorporated into the holes left in a simple inorganic structural type. The adoption of a simple salt structure for any salt containing solvent of crystallisation is unlikely, since even with the presence of the large cation and anion in **3**, a layer structure was observed.

The salts which possess more than one observed phase were shown to have similar solid state structures, the differences being attributed to small conformational differences in the ions. This phenomenon was further examined using potential energy techniques which demonstrated that the energies of the different modifications were similar but with the modification with the lowest symmetry having the lowest energy. The small differences in energy were found to be due to distinct increases in the energy of some interactions accompanied by a smaller loss in others.

Supplementary material

The following are available from the authors on request: cation–anion, cation–cation and anion–anion centroid–centroid distances for the soft salts; the calculated atomic charges used in the calculation as well as the energies listed by contact type; results for **5**.

Acknowledgements

A.L.R. thanks the British Council and the Association of Commonwealth Universities for his Commonwealth Scholarship. Thanks are also due to the A.F.O.S.R.

TABLE 2. Summary of the packing modes of the 'soft salts'

Salt	Ion	*a/c*	*CN*	Lattice type	F_s	F_c	F_d
1	$[Rh_3(\mu^3\text{-}PMe)(PMe_3)_4(CO)_5]^+$	0.99	4:5	CsCl	0.45	0.41	0 47
	$[FeRh_5(PMe_3)(CO)_{15}]^-$				0.47	0 51	0.37
2a	$[Mo_4(\mu\text{-}C_5H_4Pr^i)_4(\mu^3\text{-}S)_4]^+$	0 92	8:2	anti-fluorite	0.70	0.28	0 20
	$[Os_6(CO)_{18}]^{2-}$				0 97	0.01	0.02
2b	$[Mo_4(\mu\text{-}C_5H_4Pr^i)_4(\mu^3\text{-}S)_4]^+$	0.92	8.3/2	anti-fluorite	0.54	0 33	0.40
	$[Mo_4(\mu\text{-}C_5H_4Pr^i)_4(\mu^3\text{-}S)_4]^+$				0 69	0.29	0 20
	$[Os_6(CO)_{18}]^{2-}$				0 97	0 02	0 02
3	$[Fe_4(\mu\text{-}C_5H_5)_4(\mu^3\text{-}S)_4]^+$	0 81		layer	0.57	0 36	0 33
	$[Fe_4(NO)_4(\mu^3\text{-}S)_4]^-$				0 90	0.09	0.07
	$(CH_3)_2CO$				0.16	0 74	0 76
4	$[Fe_4(\mu\text{-}C_5H_4Me)_4(\mu^3\text{-}S)_4]^+$	0 77	6·6	anti-NiAs	0.66	0 23	0.30
	$[Fe_4(\mu\text{-}C_5H_4Me)_4(\mu^3\text{-}S)_4]^+$				0.88	0.10	0 08
	$[Fe_4(NO)_4(\mu^3\text{-}S)_4]^-$				0.93	0.06	0.05
	$[Fe_4(NO)_4(\mu^3\text{-}S)_4]^-$				0.97	0 02	0.03
5a	$[Mo_4(\mu\text{-}C_5H_4Pr^i)_4(\mu^3\text{-}S)_4]^+$	0 70	5·5	anion	0 55	0 43	0.30
	$[Fe_4(NO)_4(\mu^3\text{-}S)_4]^-$			square pyramid,	0.89	0 08	0 08
5b	$[Mo_4(\mu\text{-}C_5H_4Pr^i)_4(\mu^3\text{-}S)_4]^+$	0 70	5:5	cation	0.49	0 42	0.41
	$[Fe_4(NO)_4(\mu^3\text{-}S)_4]^-$			trigonal bipyramid	0 82	0.14	0 14

for financial support of this project. We also acknowledge the extensive use of the CHEM-X modelling system, Chemical Design Ltd, Oxford throughout this project. All the packing diagrams and ion environment diagrams presented in this work were generated by the MolDraw software [16].

References

1 M.L.H. Green, A. Hamnett, J. Qin, P Baird, J.A. Bandy, K. Prout, E. Marseglia and S.D. Obertelli, *J. Chem. Soc., Chem Commun.*, (1987) 1811.
2 P Baird, J.A. Bandy, M.L.H. Green, A. Hamnett, E. Marseglia, S.D. Obertelli, K. Prout and J. Qin, *J Chem. Soc., Dalton Trans*, (1991) 2377.
3 J. Podlahová, J. Podlaha, A. Jegorov and J. Hasek, *J Organomet. Chem*, *359* (1989) 401.
4 D L. Cocke and A. Clearfield , *Design of New Materials*, Plenum, New York, 1987
5 D Braga, F Grepioni and P. Sabatino, *J. Chem Soc, Dalton Trans*, (1990) 3137.
6 U Muller, *Acta Crystallogr., Sect B, 36* (1980) 1075.
7 D. Braga and F. Grepioni, *Organometallics, 11* (1992) 1256.
8 A.L. Rohl and D.M P. Mingos, *J Chem Soc, Dalton Trans*, (1992) 3541.
9 D.M.P. Mingos and A.L. Rohl, *J. Chem Soc, Dalton Trans.*, (1991) 3419.
10 A. Gavezzotti, *J Am. Chem Soc., 105* (1983) 5220.
11 V. Schomaker, J. Waser, R.E. Marsh and G. Bergman, *Acta Crystallogr, 12* (1959) 600.
12 D.J. Watkin and P.W. Betteridge, *SNOOPI, part of the CRYSTALS* package, Chemical Crystallography Laboratory, University of Oxford, UK.
13 E. Giglio, *Z Kristallogr., 131* (1970) 385.
14 R. Hoffmann and W.N. Lipscomb, *J. Chem. Phys., 36* (1962) 2179.
15 A.I. Kitaigorodsky, *Molecular Crystals and Molecules*, Academic Press, New York, 1973
16 J M. Cense, *Tetrahedron Comput Method, 2* (1989) 65.